DOI: 10.1002/cmdc.201100281

Identification of Small-Molecule Inhibitors of the XendoU Endoribonucleases Family

Rino Ragno,[a] Ubaldo Gioia,[b] Pietro Laneve,[c] Irene Bozzoni,[b, c] Antonello Mai,[a] and Elisa Caffarelli*[c]

The XendoU family of enzymes includes several proteins displaying high sequence homology. The members characterized so far are endoribonucleases sharing similar biochemical properties and a common architecture in their active sites. Despite their similarities, these proteins are involved in distinct RNA-processing pathways in different organisms. The amphibian XendoU participates in the biosynthesis of small nucleolar RNAs, the human PP11 is supposed to play specialized roles in placental tissue, and NendoU has critical function in coronavirus replication. Notably, XendoU family members have been implicated in human pathologies such as cancer and respiratory diseases: PP11 is aberrantly expressed in various tumors, while NendoU activity has been associated with respiratory infections by pathogenic coronaviruses. The present study is aimed at identifying small molecules that may selectively interfere with these enzymatic activities. Combining structure-based virtual screening and experimental approaches, we identified four molecules that specifically inhibited the catalytic activity of XendoU and PP11 in the low micromolar range. Moreover, docking experiments strongly suggested that these compounds might also bind to the active site of NendoU, thus impairing the catalytic activity essential for the coronavirus life cycle. The identified compounds, while allowing deep investigation of the molecular functions of this enzyme family, may also represent leads for the development of new therapeutic tools.

Introduction

The XendoU family includes several proteins from a variety of organisms ranging from viruses to humans.[1–3] So far, *Xenopus laevis* XendoU, as well as its human homologue placental protein 11 (PP11), and viral homologue NendoU, have been characterized as endoribonucleases participating in RNA-processing events. They are uridylate-specific, Mn^{2+}-dependent enzymes that produce molecules with 2′,3′-cyclic-phosphate termini, a unique characteristic of this particular class of RNases. In addition, phylogenetic and structural studies indicated that one of the most conserved regions shared by the three proteins includes the putative active site, which displays a common architecture that may be involved in different RNA processing pathways.[1] The other members of the family are annotated as putative serine proteases; nevertheless, the high evolutionary conservation with the characterized RNases suggests that they may have endoriboucleolytic activity as well.

In previous work,[4] we identified and characterized XendoU, the founding member of this family of enzymes, which is involved in the endonucleolytic processing of some intron-encoded small nucleolar RNAs (snoRNAs), a class of noncoding RNAs that play essential roles in ribosome biogenesis.[3–5] The second member to be described was a viral homologue called NendoU,[6,7] a major genetic marker of nidoviruses, which include the coronavirus causing severe acute respiratory syndrome (SARS).[2] NendoU is crucial for the viability of the viruses; mutation of a single residue within its putative active site abolishes viral RNA synthesis.[6]

Recently, the human homologue PP11 was characterized,[8] and despite its annotated function as a putative serine protease,[9] it has an endoribonuclease activity with placental tissue specificity.[8] In addition, PP11 is expressed in different tumors such as cysto-adenocarcinomas, breast cancers, testicular and gastric cancers; its dysregulated expression in tumor tissues suggests that it may be associated with carcinogenesis.[10] Due to their involvement in human pathologies, these enzymes represent potential targets for the development of therapeutic agents.

Here, we focused on the identification and validation of small molecules that may function as specific inhibitors of this class of enzymes. To this aim, we chose XendoU as a model system for several reasons: 1) its crystallographic structure is

[a] *Prof. R. Ragno,[+] Prof. A. Mai*
Dipartimento di Chimica e Tecnologie del Farmaco
Istituto Pasteur–Fondazione Cenci Bolognetti, Sapienza Università di Roma
P.le A. Moro 5, 00185 Roma (Italy)

[b] *Dr. U. Gioia,[+] Prof. I. Bozzoni*
Dipartimento di Biologia e Biotecnologie
Istituto Pasteur–Fondazione Cenci Bolognetti, Sapienza Università di Roma
P.le A. Moro 5, 00185 Roma (Italy)

[c] *Dr. P. Laneve,[++] Prof. I. Bozzoni, Dr. E. Caffarelli*
Istituto di Biologia e Patologia Molecolari
Consiglio Nazionale della Ricerche (CNR)
P.le A. Moro 5, 00185 Roma (Italy)
E-mail: elisa.caffarelli@uniroma1.it

[+] *These authors contributed equally to this work.*

[++] *Current address: Institut de Génétique et de Biologie Moléculaire et Cellulaire (IBGMC), CNRS/INSERM/ULP, B.P. 10142, 67404 Illkirch Cedex (France)*

Supporting information for this article is available on the WWW under http://dx.doi.org/10.1002/cmdc.201100281.

available[1] to be used for structure-based drug design (i.e., virtual screening); 2) the recombinant protein displays the same enzymatic features as the native enzyme;[4] 3) in vitro functional tests, distinguishing between the enzyme binding and catalytic activities, are already available.[5]

Combining multi-structure-based virtual screening with experimental analyses, we identified four compounds that specifically inhibit the catalytic activities of XendoU and PP11 in the low micromolar range. In addition, molecular docking experiments suggest that these compounds might also bind to the active site of NendoU, inhibition of which abolishes viral replication.

Results

Docking site exploration

The XendoU crystal structure revealed the presence of a phosphate bound between the α7 helix and the β-sheet III, the site crucial for catalytic activity.[1] In a tentative approach to validate the correspondence between the phosphate location and the potential catalytic site, blind docking simulations were conducted using AutoDock, as previously reported for the PP11 protein.[8] In the present docking experiments, uridine 3′-monophosphate (3′-UMP), uridine 2′,3′-cyclophosphate (2′,3′-cyclic-UMP), uracil dimer (UU), uracil trimer (UUU), and the tetramer CUUG were used in turn as substrates/ligands. Interestingly, the most favorable bound conformations predicted (i.e., the lowest energy enzyme–ligand complexes) all included the ligand docked in the proximity of the phosphate binding site (Figure 1). In particular, the predicted positions of the phosphates in 3′-UMP and 2′,3′-cyclic-UMP overlap quite well with the experimentally determined bound phosphate (Supporting Information figure S1 a–b), although the pyrimidine moiety is differently orientated. This discrepancy between predicted and experimental binding modes is probably due to the limitations of AutoDock in treating cycles as flexible. In fact, in the docking studies, 2′,3′-cyclic-UMP is conformationally constrained, and the program is unable to find alternative binding modes comparable with those of the other substrates/ligands (Figure 1). However, forcing the 2′,3′-cyclic-UMP to adopt a similar binding mode to 3′-UMP would result in a high energy complex (data not shown). Notably, the predicted bound conformations of UU, UUU and CUUG confirm the position of the active site region between the α7 helix and the β-sheet III and may explain the reported cleavage activity in the middle of a UU pair (Supporting Information figure S1 c–e).[4]

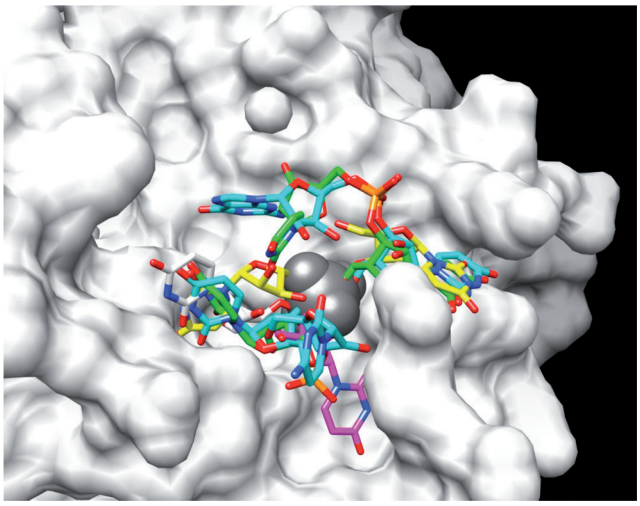

Figure 1. AutoDock proposed conformations of various XendoU substrates/ligands. 3′-UMP (light grey), 2′,3′-cyclic-UMP (magenta), UU (yellow), UUU (green) and CUUG (cyan). The van der Waals surface of XendoU is shown in white. The phosphate is shown in dark grey.

Multidocking virtual screening for the identification of potential XendoU ligands

Virtual screening, a ligand-knowledge driven approach, is now a widespread lead identification method in the pharmaceutical industry.[11,12] The best results are normally obtained by combining different virtual screening methods, using information about the drug targets as well as known ligands. Unfortunately, no information regarding known ligands was available in the present study; therefore, a multidocking approach was used (consensus docking). This method was applied to a database of 1990 compounds listed in the US National Cancer Institute (NCI) diversity set, a library that is representative of a larger collection of approximately 140000 chemicals. Among the available docking programs,[13] attention was focused on free academic programs and, from among them, AutoDock,[14] DOCK,[15] SURFLEX[16] and OMEGA/FRED[17] were selected on the basis of both different implemented docking algorithms and successful validations.[18] Unlike the protocol reported by Miteva et al.,[18] the consensus docking protocol used here (see Experimental Section for details) was conducted using the four docking methods in parallel, and a consensus score was applied to rank the overall obtained poses (Supporting Information figure S2).

Identification of specific inhibitors of XendoU cleavage activity

The multidocking approach allowed us to select 40 compounds with potential inhibitory function from over 1990 molecules listed in the NCI diversity set. These compounds were experimentally tested for their biological activity using an in vitro cleavage assay.[5] A typical assay was carried out by incubating the enzyme with its RNA substrate in the presence of manganese, and by analyzing the products of cleavage at different times during the incubation.[5] For this reaction, the U16 snoRNA primary transcript (003 RNA), mimicking the natural XendoU substrate, was used.[19] As a source of enzymatic activity, we used a recombinant version of XendoU, the N-terminal hexahistidine-tagged XendoU (His-XendoU), which displays the same biochemical features as the native enzyme.[5] The cleavage assay was carried out in 10% DMSO, a concentration that allowed compound solubility without affecting XendoU cleavage activity (data not shown). Figure 2a shows the cleavage reactions carried out in the presence of the seven best perform-

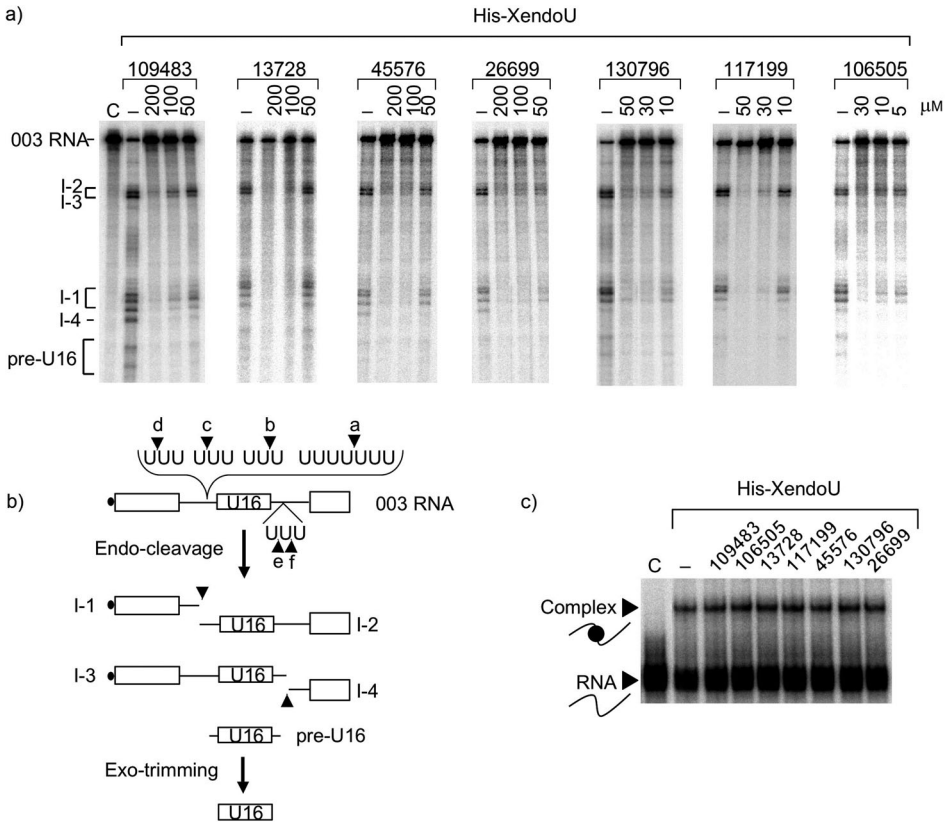

Figure 2. Functional validation of XendoU inhibitors **1**–**7**. a) XendoU processing activity was analyzed in the presence of the best performing individual compounds (indicated above each lane). ^{32}P-labeled 003 RNA was incubated with His-XendoU alone (lanes –) or in the presence of decreasing amounts of inhibitors, at the specific concentrations. Untreated sample (input RNA) was fractionated in lane C. b) Schematic representation of U16 snoRNA processing. U16 primary transcript (003 RNA) as well as the complementary cleavage products (I-1 and I-2; I-3 and I-4) released by XendoU endonucleolytic clevages upstream (a, b, c and d sites) and downstream (e and f sites) of the U16 snoRNA are depicted. The double cleavage upstream and downstream of the U16-coding region produces pre-U16 molecules that, in the cell system, are converted by exonuclease trimming to the mature snoRNA. c) XendoU binding activity was tested in the presence of inhibitors. His-XendoU was incubated with a fixed amount of ^{32}P-labeled mini 003 RNA alone (lane –) or in the presence of each compound at a concentration of 200 μM. RNA incubated in buffer alone was loaded in lane C. Arrowheads point to free RNA (RNA) and protein/RNA complex (Complex).

ing agents (**1**–**7**), affecting XendoU activity at different micromolar concentrations.

NSC 13728 (**1**), NSC 45576 (**3**) and NSC 109483 (**5**) almost completely abolished endoribonucleolytic activity at the higher concentration of 200 μM, as demonstrated by the absence of the specific cleavage products I-1, I-2, I-3 and I-4 (Figure 2a–b). Notably, NSC 26699 (**2**), NSC 106505 (**4**), NSC 117199 (**6**) and NSC 130796 (**7**) inhibited the activity at lower concentrations (100 μM for **2**; 50 μM for **6** and **7**; 30 μM for **4**; Figure 2a and Table 1). The same analysis, performed on a shorter RNA substrate (21-nucleotide-long oligoribonucleotide P1) that contains two XendoU cleavage sites,[4] confirmed the inhibitory effect of compounds **1**–**7** and indicated that such activity does not depend on the length of the RNA substrate (Supporting Information figure S3). In addition, to exclude the possibility that these compounds interact nonspecifically with the His-tag of the recombinant protein, an RNA-processing assay was carried out in *X. laevis* oocyte nuclear extract (ONE) containing XendoU native enzyme.[4] The results obtained with one of the most active compounds, NSC 130796 (**7**), confirmed that the inhibitory activity is independent of the presence of the His-tag (Supporting Information figure S4).

To determine whether the seven identified inhibitors (**1**–**7**) interfere with XendoU cleavage and/or binding activity, we tested their ability to hamper XendoU–RNA interactions. An in vitro binding assay was carried out using the recombinant enzyme His-XendoU and the mini-003 RNA substrate, a shorter version of 003 RNA. We chose this RNA substrate since its length allows the formation of stable RNA–protein complexes.[5] Recombinant XendoU was incubated with radiolabeled mini-003 RNA in the absence or presence of a fixed concentration (200 μM) of each inhibitor. The assembled complex was then visualized in an electrophoretic mobility shift assay. As shown in Figure 2c, the percentage of shifted RNA, representing the RNA fraction assembled with the protein, was not affected by the presence of the inhibitors, suggesting that these compounds do not influence RNA–protein interaction.

To establish whether the action of compounds **1**–**7** is selective, we tested them on unrelated endoribonucleases, RNase A and RNase T1, which specifically degrade single-stranded RNAs at cytosine and uracil or guanine, respectively. The enzymes were incubated with radiolabeled P1 RNA substrate in the presence of test compound at a maximum concentration of 200 μM. The results show that neither RNase A nor RNase T1 activity were affected by high drug concentrations (Supporting Information figure S5), thus implying selectivity.

Binding-mode analysis of the active hits in XendoU

The predicted binding modes of the seven XendoU inhibitors (**1**–**7**) identified from the library of 40 compounds were visually inspected. The binding modes predicted by the four docking programs used in the virtual screening protocol were in good agreement with one another (Figure 3). It is noteworthy that a lower half maximal inhibitory concentration (IC_{50}) value correlates to improved agreement between the four predicted bind-

Table 1. Structures of compounds **1**–**7** and their biological activities (IC_{50}) against XendoU cleavage.

Compd		IC_{50} [μM]
NSC 13728 (**1**)	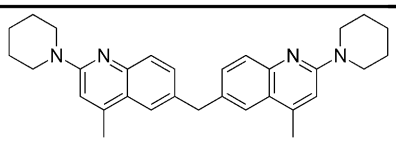	40
NSC 26699 (**2**)	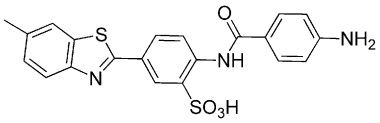	20
NSC 45576 (**3**)	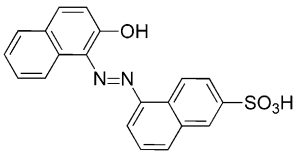	29
NSC 106505 (**4**)	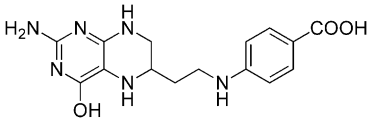	2.8
NSC 109483 (**5**)	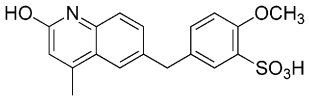	23
NSC 117199 (**6**)	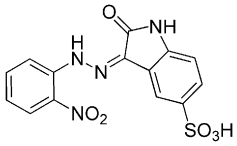	5.7
NSC 130796 (**7**)	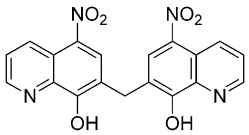	6.4

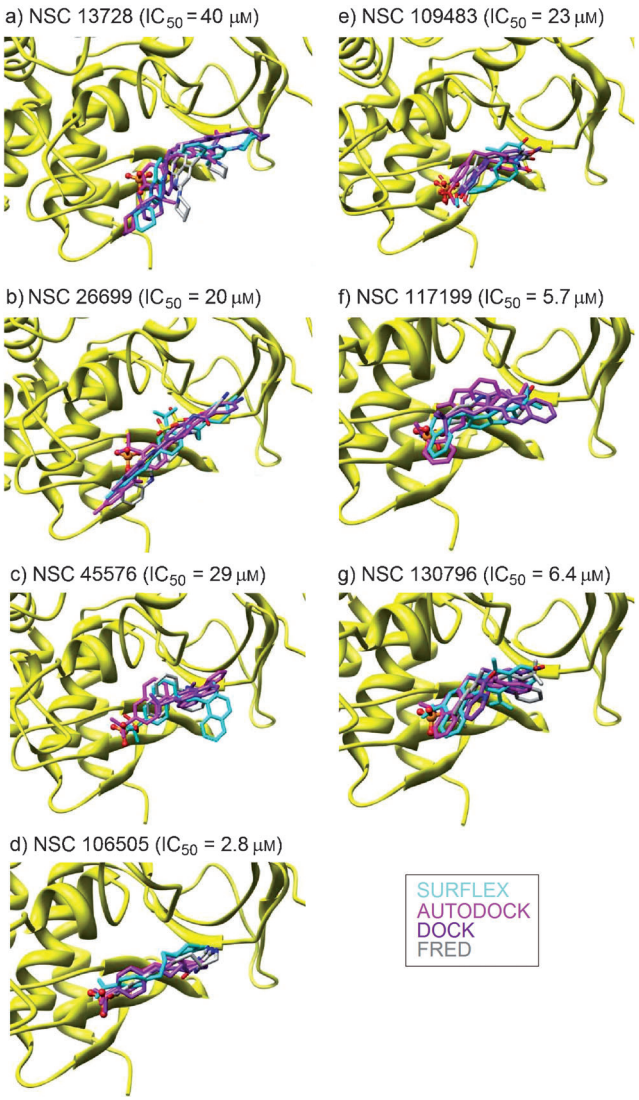

Figure 3. Docked conformations of the XendoU inhibitors. A portion of the XendoU enzyme is displayed as a yellow ribbon. Surflex, AutoDock, Dock and FRED overlapped poses of a) NSC 13728 (**1**), b) NSC 26699 (**2**), c) NSC 45576 (**3**), d) NSC 106505 (**4**), e) NSC 109483 (**5**), f) NSC 117199 (**6**) and g) NSC 130796 (**7**) are shown, and their IC_{50} values are given.

ing conformations for each hit compound. In fact, increasing conformational disorder is associated with decreased inhibitory activity. This is in agreement with the observation that tighter interactions are predicted between the enzyme and inhibitor for NSC 106505 (**4**), NSC 117199 (**6**) and NSC 130796 (**7**), whereas the weakest interactions are predicted to be formed by the least active compound, NSC 13728 (**1**). Subsequent energy calculations indicated that the docked conformations proposed by AutoDock display the lowest energies, and consequently, we used this program for further analysis. Ligplot[20] diagrams of the AutoDock poses for inhibitors **1**–**7** show an extended network of predicted interactions for the most active molecules (**4**, **6** and **7**); this network is reduced with the other inhibitors, with NSC 13728 (**1**; least active agent) predicted to have the least number of interactions (Supporting Information figure S6). A three-dimensional analysis of the AutoDock predicted binding modes led to the definition of specific areas that are associated with the inhibitory activity of compounds **1**–**7** (Supporting Information figure S7). The extended hydrophobic ligand–receptor interactions (purple areas in Supporting Information figure S8) in the less active compounds seem to compensate for the lack of strong interactions (compare ligplot diagrams in Supporting Information figure S6). Such an interaction profile allowed us to define ligand surfaces that are important for XendoU inhibition. In particular, the analysis of each molecular feature for all the identified hits led to the definition of a pharmacophore model made by six points that describe the minimal chemical characteristics required for XendoU inhibition (Figure 4); four of them, namely HY-1, HY-2, HA-1 and HA-2, are derived from the most active inhibitors and two of them, HY-3 and HY-4, are related to the less potent compounds.

The hydrophobic feature HY-1 is present in all seven compounds and can be considered the core of the pharmacophore scaffold. Although it does not make important interactions with any XendoU residues, HY-1 is connected to HA-1, an hydrogen acceptor that is missing only in the least active compound (NSC 13728). HA-1 is an oxygen atom in nitro or sulfone

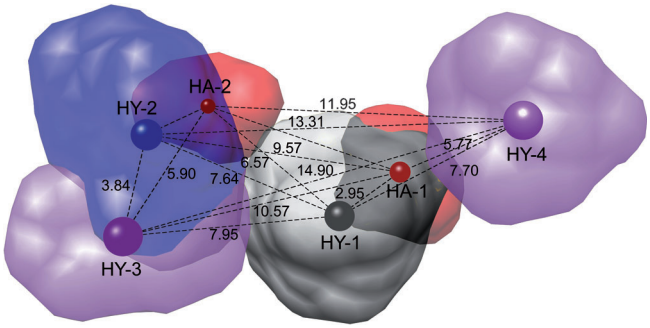

Figure 4. Pharmacophore model derived from XendoU inhibitors. The surfaces derived from the most active compounds (**4**, **6** and **7**) are colored in red, blue and grey. The peculiar areas from the less active agents (**1**–**3** and **5**) are depicted in purple. The hydrophobic features (HY-1, −2, −3 and −4) and the hydrogen acceptors (HA-1 and −2) are also indicated. Interaction (——) distances are given in angstroms (Å).

groups and overlaps with the phosphate found in the XendoU crystal structure.[1] HA-1 is mainly involved in electrostatic-type interactions (i.e., hydrogen bond) and is predicted to bind in a pocket formed by charged residues (Arg 149, His 162, Asn 270, His 272 and Thr 278; Supporting Information figures S7 and S8). HY-2 is the second hydrophobic feature comprising aromatic and nitrogen-containing aromatic rings; this feature is present in compounds **1**, **3**–**7** but only partially present in NSC 26699 (**2**), where the benzothiazole benzene ring is shifted away from the other aromatic rings. HY-2 is slightly larger than HY-1 and is involved in hydrophobic interactions in a large pocket formed by the side chain portions of His 178, Lys 224, Pro 225 and Tyr 280. The fourth main feature, HA-2, is present in only the most active compounds and represents oxygen atoms in nitro (NSC 117199 and NSC 130796) or pyrimidinone-like ring (NSC 106505). HA-2 is found with hydrogen-bonding distance from His 178 ε-nitrogen. HY-3 is the first supplementary feature, specific to weakly active NSC 26699 (**2**) and NSC 45576 (**3**), and it is represented by aromatic moieties filling a hydrophobic pocket formed by Met 174, Trp 219 and Lys 224 side chains. The last feature, HY-4, is present in only the less active compounds and defined by the pyridine and aniline of NSC 13728 (**1**) and NSC 26699 (**2**), respectively. HY-4 occupies a small pocket delimited by portions of Lys 252, Asn 270, Arg 271 and His 272 residues.

Investigation of human and viral PP11 inhibition by the active compounds

To further extend our investigation to other members of the XendoU family, we monitored the effect of inhibitors **1**–**7** on the human homologue PP11. The recombinant enzyme, His-PP11,[8] was incubated with the radiolabeled 21-nucleotide-long P1 RNA substrate[4] in the presence of each compound at a maximum concentration of 200 μM.

As shown in Figure 5a, four of the seven molecules: NSC 13728 (**1**), NSC 45576 (**3**), NSC 106505 (**4**) and NSC 130796 (**7**), inhibited PP11-processing activity. The inhibitory activity of these compounds was further investigated at lower concentrations. As shown in Figure 5b, NSC 130796 (**7**) displayed the strongest inhibitory activity (IC_{50} = 29 μM determined by six concentrations from 5 to 200 μM). As for XendoU, a mobility shift assay showed that the active compounds only impair the catalytic activity of PP11 (Figure 5c). Finally, we investigated the possible binding mode of the four active PP11 inhibitors: NSC 13728 (**1**), NSC 45576 (**3**), NSC 106505 (**4**) and NSC 130796 (**7**). AutoDock was applied on the recently reported PP11 homology model.[8] Similar to what we observed for XendoU by blind docking procedure, the poses of the four inhibitors overlap in the same region (Figure 5d). Notably, the identified binding area coincides with the previously reported PP11 active site region.[8] The interaction profiles of the four inhibitors are reported in the ligplot diagrams in Supporting Information figure S9.

Due to structural similarities between the XendoU family members and the availability of further structural information, we extended our docking protocol to include the viral homologue NendoU (PDB: 2H85).[21] We checked for binding mode analogies of inhibitors **1**, **3**, **4** and **7** that were active against both XendoU and PP11 enzymes. Strikingly, the blind docking (AutoDock) procedure performed on NendoU positioned all four compounds in the same XendoU/PP11 binding region, corresponding to the active site (Figure 6a–b). Furthermore, the binding conformation of NSC 130796 (**7**)—one of the most active compound against both XendoU and PP11—into NendoU was very similar to that observed with the other two proteins, even though the three orientations were not fully superimposable (Figure 6c).

Discussion

Endoribonucleases are considered key players in all general processes associated with eukaryotic RNA metabolism in various subcellular compartments, where they are involved both in degradation pathways, such as RNA turnover, and in maturation pathways, producing functional RNA molecules.[22] XendoU is an endoribonuclease we discovered and purified from *X. laevis* oocyte.[4] Characterization of its activity indicated that, in *X. laevis* germ cells, it is responsible for the release of the intron-encoded U16 and U86 snoRNAs from their primary transcripts. These small noncoding RNAs are required for rRNA modifications that are, in turn, essential for ribosome biogenesis and function. However, whether XendoU plays different or additional functions in somatic cells is still unexplored. Subsequent production of recombinant XendoU protein allowed us to further characterize its activity by pursuing biochemical and structural studies. The three-dimensional structure of XendoU was solved, and the description of its active site, compared with those of other RNA processing enzymes, indicated that it displays a unique fold.[1]

XendoU has been proposed as the founding member of a previously unidentified protein family.[2,5] Phylogenetic analyses highlighted that XendoU is conserved among higher eukaryotes, with homologues from nidoviruses and a cyanobacterium also.[1] Despite the high conservation of the active site architecture, the endoribonucleolytic function has been proved

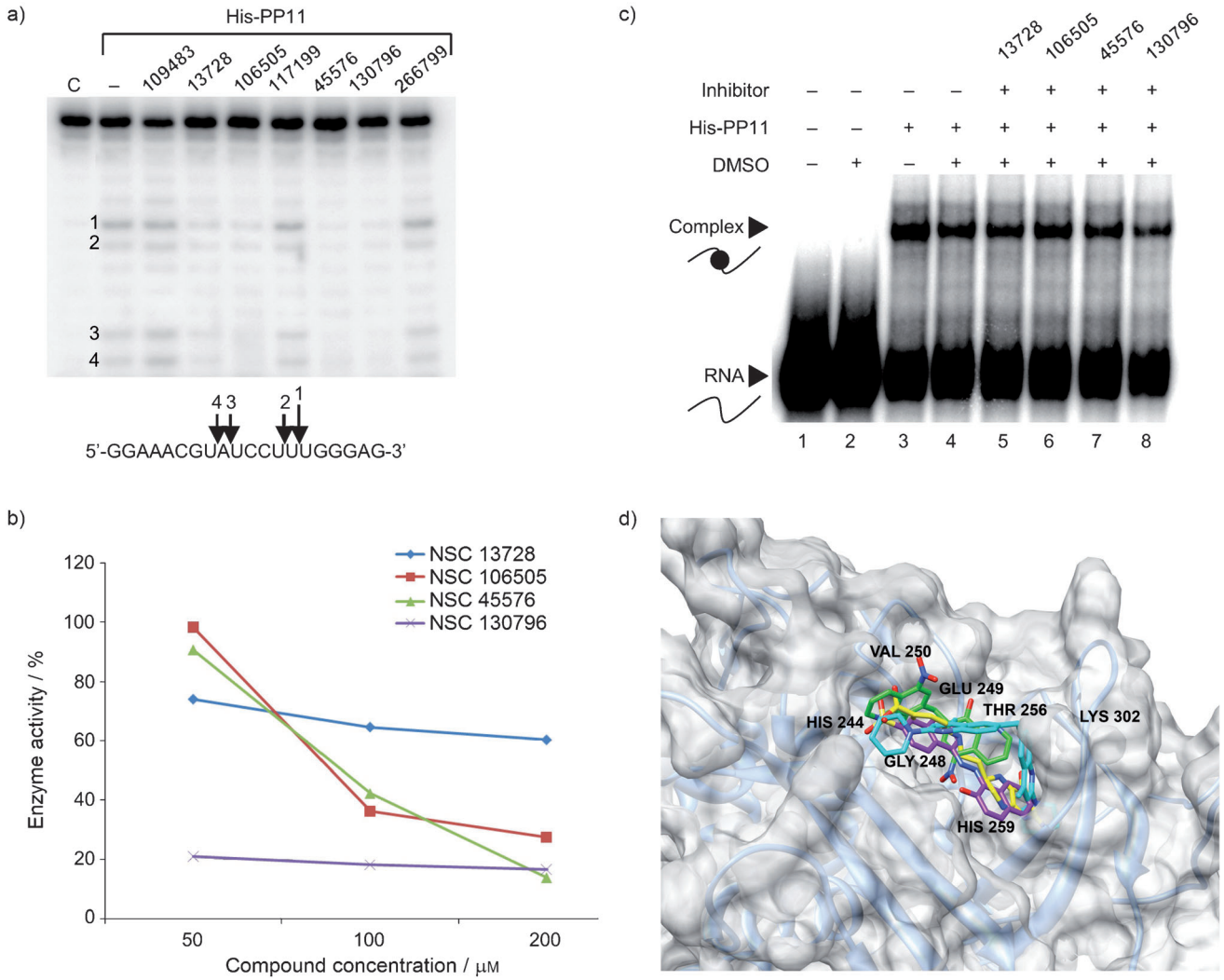

Figure 5. Analysis of inhibition of human PP11. a) Cleavage assay: in vitro processing reaction was performed by incubating 5′-end-labeled P1 oligoribonucleotide (run as untreated molecule in lane C) with His-PP11 alone (lane –) or in the presence of each inhibitor at a concentration of 200 μM. The sequence of P1 oligoribonucleotide, as well as the PP11 cleavage sites (indicated by arrows), are reported below. b) Dose-dependent inhibition assay of the four PP11 inhibitors. c) Binding assay: the four compound (**1**, **3**, **4** and **7**) that inhibit PP11 cleavage activity were further tested for their ability to affect PP11 binding properties. A mobility shift assay was performed as already described for XendoU. His-PP11 was incubated with a fixed amount of ^{32}P-labeled RNA alone (lanes 3 and 4) or in the presence of each compound at a concentration of 200 μM (lanes 5–8). Untreated RNA was fractionated in lanes 1 and 2. The arrows point to the RNA–protein complex (Complex) or to the free RNA (RNA). d) Docked conformations of the PP11 inhibitors: NSC 13728 (**1**; cyan), NSC 45576 (**3**; purple), NSC 106505 (**4**; yellow), NSC 130796 (**7**; green). The van der Waals surface of PP11 is shown in white.

for only three members of the family, whereas the other members, annotated as putative serine proteases, are still uncharacterized. The human and viral enzymes have been linked to human pathologies, such as tumors and respiratory diseases; therefore, the identification of small molecules that specifically interfere with such activities may represent the first step toward the development of novel therapeutic treatments.

We took advantage of our experience with XendoU[1,5] to set up a virtual screening approach allowing us to select, from the NCI diversity set, small molecules potentially endowed with enzyme inhibitory function. We reasoned that the main characteristic of such molecules should be their ability to locate inside the conserved active site.[1,8] A preliminary docking simulation using AutoDock was applied to XendoU using various known substrates. This method confirmed the location of the XendoU active site in the region between the α7 helix and the β-sheet III that we previously determined through biochemical and crystallographic approaches.[1,5] In a second step, virtual screening was achieved by a multidocking approach derived from the combination of AutoDock with other docking methods. Such an approach, applied to the NCI diversity set, led to the selection, from over 1990 molecules, of 40 compounds displaying potential inhibitory features. These molecules were experimentally tested on both *X. laevis* and human recombinant enzymes. Only four inhibitors effectively impaired the catalytic activity of both endoribonucleases, while not affecting the enzyme–substrate interaction. These results, while supporting our previous conclusion that the XendoU RNA binding and

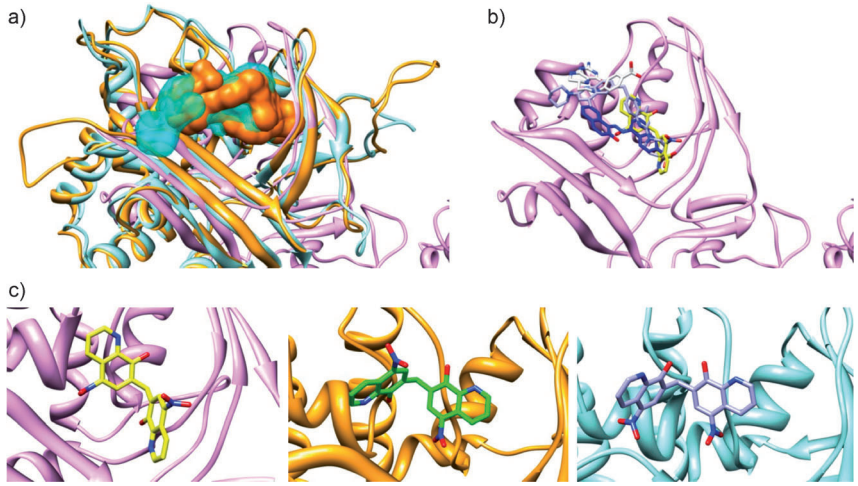

Figure 6. Binding mode comparisons of the XendoU/PP11 common, active compounds docked in the three RNAses. a) NendoU (pink), XendoU (cyan) and PP11 (orange) cumulative binding surfaces of the XendoU/PP11 common inhibitors (NCS 130796, NCS 106505, NCS 45576 and NSC 13728). b) AutoDock proposed binding conformations of the XendoU/PP11 active compounds into the NendoU opened form (PDB: 2H85[21]): NSC 13728 (**1**; purple), NCS 45576 (**3**; blue), NCS 106505 (**4**; white), NCS 130796 (**7**; yellow). c) Binding mode comparison of NCS 130796 (**7**) docked in NendoU (pink), PP11 (orange) and XendoU (cyan).

processing activities are functionally separated,[5] revealed that the compounds bind to the active site. Such conclusions will be further confirmed by co-crystallization of the most effective inhibitors with the XendoU enzyme.

It is noteworthy that we found a good agreement between the experimental and virtual screening data. In fact, molecules displaying the highest inhibitor activity against XendoU, namely NSC 106505 (**4**), NSC 117199 (**6**) and NSC 130796 (**7**), are those establishing the most extended network of interactions; accordingly, the less active compounds displayed a reduced number of interactions. Exploitation of XendoU inhibitor characteristics allowed us to produce a pharmacophore model that, carrying the essential features required for inhibiting the enzymatic activity, represents the first step in the design of new molecules as inhibitors of the entire XendoU family.

Our study was also extended to the other characterized member of the XendoU family, the viral NendoU enzyme. Although no experimental evidence is yet available, the docking simulations positioned the four active compounds in the NendoU region corresponding to its active site.[21] This result was not unexpected since the catalytic domain, shared by the three enzymes, is conserved in structure and sequence and suggests that the XendoU/PP11 inhibitors reported here could also act as coronavirus NendoU inhibitors and, thus, as potential antiviral compounds, which could interfere with the infectious virus life cycle.

A mandatory requirement for inhibitors is specificity. We demonstrated that this feature is fully accomplished by the selected compounds, since they do not affect the catalytic activity of other endoribonucleases, such as RNases A and T1, even at high concentration.

Conclusion

The observation that the selected molecules localize in the conserved active site of the three endoribonucleases opens new perspectives for further investigations aimed at predicting the active site and unveiling the function of other members of the XendoU family, which may be flexibly involved in crucial RNA processing pathways. Moreover, due to their substrate specificity, the inhibitors identified here could also represent lead compounds for the development of new candidate antiviral agents.

Experimental Section

Computational procedures

Protein preparation: Three enzyme monomers were present in the XendoU coordinates retrieved from the protein databank (PDB: 2C1W[1]), and within them, the putative phosphate binding site residue Arg 149 exhibited two different side chain conformations. Together, this information gives six different XendoU conformations. Due to steric hindrance that is generated upon hydrogen atom addition, the six XendoU structures where geometrically optimized using the AMBER 8 molecular modeling suite. To this aim, the structures were solvated (SOLVATEOCT command) in a box extending 10 Å with ~8000 water molecules (TIP3 model) and neutralized with Na^+ ions. The solvated complexes were then refined by minimization (5000 interactions) using the SANDER module of AMBER. Graphical inspection of the minimized models and images were produced using the University of California, San Francisco (UCSF) Chimera package (version 1.5.2) from the Resource for Biocomputing, Visualization, and Informatics at UCSF (supported by the US National Institutes of Health, grant: P41 RR001081).[23] The atom charges assigned on the protein by the leap modules were maintained for the subsequent docking simulations. The same protocol was used for NendoU, while the structure of PP11 was prepared as described earlier.[8] For the subsequent docking simulations, all six XendoU conformations were used (cross docking), thus including protein mobility to some extent in the docking.

Ligand preparation: The structures of 3′-UMP, 2′,3′-cyclic-UMP, UU, UUU and CUUG were prepared starting from ASCII text, using the standalone version of PRODRG (version 2.0), in conjunction with the GROMACS suite (version 3.3.1). For virtual screening, the US National Cancer Institute diversity set (http://dtp.nci.nih.gov), a database consisting of over 1990 compounds, was used.

AutoDock: Docking was performed using AutoDock (version 3.0.5) as previously reported.[8] For each compound, the proposed poses were clustered as described in the AutoDock manual. For the substrate dockings, a grid that embraced the whole XendoU protein was used and centered to the protein mass center. For virtual

screening, a smaller grid was used comprising all the protein residues within 10 Å of the experimentally determined XendoU-bound phosphate, and the grid was centered on the phosphorous atom of the phosphate group. A total of 150 runs were performed for each enzyme.

DOCK: Version 5.4 was used. DOCK applies a sphere-matching algorithm to fit ligand atoms to spheres in the binding pocket. SPHGEN (included in DOCK 5.4) was used to create overlapping spheres within a radius of complementarity to the protein surface. A Connolly surface of each binding pocket was generated using DMS (included in DOCK 5.4) with a probe radius of 1.4 Å. The binding pocket included all receptor residues at a distance of 10 Å from any atom of the XendoU-bound phosphate. An example DOCK input file is given in table S1 of the Supporting Information.

SURFLEX: This program (version 1.22)[24] is the implementation of the Hammerhead methodology described by Welch et al.[25] Similar to its predecessor, it generates a pseudo-binding site (called a protomol), and then fragments each individual ligand that is aligned with the protomol, in order to yield poses that maximize molecular complementarity with the binding site. Definition of the protomol is a sensitive step, and the docking performance depends on the area considered to form the binding site and how far from a potential ligand the site should extend, as well as how deep into the protein the atomic probes used to define the protomol can penetrate. Here, the protomol was generated using a XendoU protein subset comprising all residues within 10 Å from the bound phosphate.

OMEGA/FRED: FRED (version 2.1.1) requires a set of low-energy conformations for each ligand. The conformers were generated using OMEGA (version 1.8.1) and stored in a single binary file. For the conformation generation settings, see table S2 in the Supporting Information. FRED docking consists of four steps: exhaustive docking, optimization, consensus structure, and optional force-field refinement. During exhaustive docking, a pose ensemble is generated by rigidly rotating and translating each conformer within the active site. The active site was defined by a box of 10 Å (default) extension in all directions from the XendoU-bound phosphate. The detailed docking setup is reported in table S3 of the Supporting Information.

Consensus docking/scoring: The top scoring poses for each molecule in each docking experiment were compared by means of a root mean square deviation (rmsd) of atom position and ranked in order, with compounds having the lowest rmsd values ranking the highest (consensus docking). A comparison of the scorings in each docking-program-related scoring function was performed by simple addition of the rank orders in each docking (consensus docking) and reordering the compounds from lowest to highest total rank. Finally, by summing the rank order in the two consensus docking procedures, the final rank was obtained. The top 40 ranked molecules were then selected and obtained from the US National Cancer Institute (see table S4 of the Supporting Information).

Biology

Preparation of inhibitors: The inhibitors were dissolved in DMSO (20%) to give a final concentration of 400 μM. According to the experimental requirements, they were diluted in the same solvent to ensure a fixed concentration of 10% DMSO in each reaction mixture.

In vitro RNA transcription: The 003 and mini-003 RNAs (described in Reference [3]) were synthesized by in vitro transcription in the presence of [α-^{32}P]UTP according to a literature protocol.[26]

Processing assay: 3×10^4 cpm of ^{32}P-labeled precursor (corresponding to 2 fmol) were incubated with 10 ng of purified His-XendoU in 5 mM $MnCl_2$, 50 mM NaCl, 25 mM Hepes, pH 7.5, 1 mM dithiothreitol, 10 μg of *Escherichia coli* tRNA, 20 U of RNase inhibitor (GE Healthcare) and 10% DMSO in the presence of decreasing amounts (ranging from 200 to 2.5 μM) of specific inhibitors for 30 min at 24 °C. In parallel, RNA processing assay was also carried out in *Xenopus laevis* oocyte nuclear extract (ONE), containing XendoU native enzyme,[4] in the presence of NSC 130796 (**7**), active against both XendoU and PP11.

Reaction products were extracted and analyzed on 6% polyacrylamide 7 M urea gels (29:1 acrylamide/bis). P1 oligoribonucleotide (5′-GGAAACGUAUCCUUUGGGAG-3′) was 5′-end labeled with [α-^{32}P]ATP (PerkinElmer Life Sciences) and incubated with 100 ng of His-PP11, 100 ng His-XendoU, or 2 ng of RNase A, using the conditions described above. Reaction products were analyzed on 20% polyacrylamide 7 M urea gels. For RNase T1 assay, labeled P1 substrate was incubated for 30 min at 24 °C with 0.04 U μL^{-1} of enzyme in 2 mM EDTA, 50 mM Tris/HCl, pH 7 and 10% DMSO.

Binding reaction: Binding assays were performed by incubating 2 fmol of [α-^{32}P]UTP (PerkinElmer Life Sciences) in vitro transcribed mini 003 RNA with 40 ng of recombinant proteins (XendoU or PP11) in a final volume of 10 μL binding buffer (10 mM Hepes, pH 7.5, 75 mM NaCl, 20 mM ethylene glycol tetraacetic acid (EGTA), 1 mM dithiothreitol, 20% glycerol, 20 U RNase inhibitor and 10% DMSO). After 30 min incubation at 24 °C, the RNA–protein complexes were fractionated on 8% polyacrylamide native gels (29:1 acrylamide:bis) containing 4% glycerol and visualized by autoradiography.

IC_{50} calculations: The inhibitory activity of the individual compounds was evaluated as percentage of uncleaved RNA substrate versus the input RNA and expressed as half maximal inhibitory concentration (IC_{50}). The IC_{50} values were determined by nonlinear fitting strategies performed using PRISM (version 5.0) (GraphPad SoftWare Inc., San Diego, CA, USA).

Acknowledgements

We thank C. Bourgeois for critical reading of the manuscript. We also thank M. Arceci for technical help. This work was supported by the European Union SIROCCO project (LSHG-CT-2006–07900), the European Science Foundation NuRNASu project , the Associazione Italiana per la Ricerca sul Cancro, the Italian Progetti di Ricerca di Interesse Nazionale, the Centro di Eccellenza Biologia e Medicina Molecolare (Rome, Italy), and the Fondazione Roma (Italy). U.G. was supported by a fellowship from the Fondazione Italiana per la Ricerca sul Cancro.

Keywords: AutoDock · endoribonucleases · RNA processing · structure-based drug design · XendoU family

[1] F. Renzi, E. Caffarelli, P. Laneve, I. Bozzoni, M. Brunori, B. Vallone, *Proc. Natl. Acad. Sci. USA* **2006**, *103*, 12365 – 12370.

[2] E. J. Snijder, P. J. Bredenbeek, J. C. Dobbe, V. Thiel, J. Ziebuhr, L. L. M. Poon, Y. Guan, M. Rozanov, W. J. M. Spaan, A. E. Gorbalenya, *J. Mol. Biol.* **2003**, *331*, 991 – 1004.

[3] E. Caffarelli, M. Arese, B. Santoro, P. Fragapane, I. Bozzoni, *Mol. Cell. Biol.* **1994**, *14*, 2966 – 2974.
[4] P. Laneve, F. Altieri, M. E. Fiori, A. Scaloni, I. Bozzoni, E. Caffarelli, *J. Biol. Chem.* **2003**, *278*, 13026 – 13032.
[5] U. Gioia, P. Laneve, M. Dlakic, M. Arceci, I. Bozzoni, E. Caffarelli, *J. Biol. Chem.* **2005**, *280*, 18996 – 19002.
[6] K. A. Ivanov, T. Hertzig, M. Rozanov, S. Bayer, V. Thiel, A. E. Gorbalenya, J. Ziebuhr, *Proc. Natl. Acad. Sci. USA* **2004**, *101*, 12694 – 12699.
[7] K. Bhardwaj, J. Sun, A. Holzenburg, L. A. Guarino, C. C. Kao, *J. Mol. Biol.* **2006**, *361*, 243 – 256.
[8] P. Laneve, U. Gioia, R. Ragno, F. Altieri, C. Di Franco, T. Santini, M. Arceci, I. Bozzoni, E. Caffarelli, *J. Biol. Chem.* **2008**, *283*, 34712 – 34719.
[9] U. Grundmann, J. Romisch, B. Siebold, H. Bohn, E. Amann, *DNA Cell Biol.* **1990**, *9*, 243 – 250.
[10] N. Inaba, H. Ishige, M. Ijichi, N. Satoh, R. Ohkawa, S. Sekiya, S. Shirotake, H. Takamizawa, T. Renk, H. Bohn, *Oncodev. Biol. Med.* **1982**, *3*, 379 – 389.
[11] I. Muegge, *Mini-Rev. Med. Chem.* **2008**, *8*, 927 – 933.
[12] D. V. Green, *Prog. Med. Chem.* **2003**, *41*, 61 – 97.
[13] S. F. Sousa, P. A. Fernandes, M. J. Ramos, *Proteins* **2006**, *65*, 15 – 26.
[14] G. M. Morris, R. Huey, A. J. Olson, *Curr. Protoc. Bioinformatics* **2008**, Unit 8.14; DOI: 10.1002/0471250953.bi0814s24.
[15] D. T. Moustakas, P. T. Lang, S. Pegg, E. Pettersen, I. D. Kuntz, N. Brooijmans, R. C. Rizzo, *J. Comput.-Aided Mol. Des.* **2006**, *20*, 601 – 619.
[16] A. N. Jain, *J. Comput.-Aided Mol. Des.* **2007**, *21*, 281 – 306.
[17] G. B. McGaughey, R. P. Sheridan, C. I. Bayly, J. C. Culberson, C. Kreatsoulas, S. Lindsley, V. Maiorov, J. F. Truchon, W. D. Cornell, *J. Chem. Inf. Model.* **2007**, *47*, 1504 – 1519.
[18] M. A. Miteva, W. H. Lee, M. O. Montes, B. O. Villoutreix, *J. Med. Chem.* **2005**, *48*, 6012 – 6022.
[19] E. Caffarelli, P. Fragapane, I. Bozzoni, *Biochem. Biophys. Res. Commun.* **1992**, *183*, 680 – 687.
[20] A. C. Wallace, R. A. Laskowski, J. M. Thornton, *Protein Eng.* **1995**, *8*, 127 – 134.
[21] S. Ricagno, M. P. Egloff, R. Ulferts, B. Coutard, D. Nurizzo, V. Campanacci, C. Cambillau, J. Ziebuhr, B. Canard, *Proc. Natl. Acad. Sci. USA* **2006**, *103*, 11892 – 11897.
[22] R. Tomecki, A. Dziembowski, *RNA* **2010**, *16*, 1692 – 1724.
[23] UCSF Chimera, http://www.cgl.ucsf.edu/chimera; E. F. Pettersen, T. D. Goddard, C. C. Huang, G. S. Couch, D. M. Greenblatt, E. C. Meng, T. E. Ferrin, *J. Comput. Chem.* **2004**, 25, 1605 – 1612.
[24] A. N. Jain, *J. Med. Chem.* **2003**, *46*, 499 – 511.
[25] W. Welch, J. Ruppert, A. N. Jain, *Chem. Biol.* **1996**, *3*, 449 – 462.
[26] D. A. Melton, P. A. Krieg, M. R. Rebagliati, T. Maniatis, K. Zinn, M. R. Green, *Nucleic Acids Res.* **1984**, *12*, 7035 – 7056.

Received: June 4, 2011
Published online on July 29, 2011

